A Multichannel Oscillator for a Resonant Chemical Sensor System

Hyunjoo Jenny Lee, *Member, IEEE*, Kwan Kyu Park, *Member, IEEE*, Ömer Oralkan, *Senior Member, IEEE*, Mario Kupnik, *Senior Member, IEEE*, and Butrus T. Khuri-Yakub, *Fellow, IEEE*

***Abstract*—Vapor detection using highly sensitive miniaturized resonant sensors is of great interest for many applications, including consumer, industrial, and environmental applications. An operational-amplifier-based multichannel oscillator that interfaces with a 50-MHz capacitive micromachined ultrasonic transducer array is presented for chemical sensing applications. The circuit was implemented in a 0.18-μm CMOS technology to reduce power consumption, number of wires, and active area per channel. The presented integrated circuit also addresses the potential-frequency-locking problem between channels by allowing the open-loop gain to be adjustable off-chip. The feasibility of the developed oscillator for the chemical sensing application is demonstrated. Two channels that were operated simultaneously achieved excellent volume sensitivities of $8.5 \times 10^{-4}\%/\text{Hz}$ and $3.9 \times 10^{-4}\%/\text{Hz}$, respectively, to relative humidity in N_2.**

***Index Terms*—Capacitive micromachined ultrasonic transducer (CMUT), chemical sensor, humidity detection, multichannel oscillators.**

I. Introduction

THE DEMAND for microelectromechanical systems (MEMS)-based miniaturized chemical sensors is continuously increasing in a wide range of applications because of their small size, low power consumption, and CMOS compatibility [1]–[5]. Potential applications span across many fields, such as industrial, environmental, medical, automotive, and consumer applications. Micromachined resonant devices that are based on the mass-loading effect are promising platforms for miniaturized chemical sensor systems. They offer superior sensitivity, high resolution, and a wide dynamic range (Fig. 1) [6]. These devices include thin film bulk acoustic resonators (FBARs) [7], surface acoustic waves (SAWs) [8], capacitive micromachined ultrasonic transducers (CMUTs) [9], and micromachined cantilevers [10], [11].

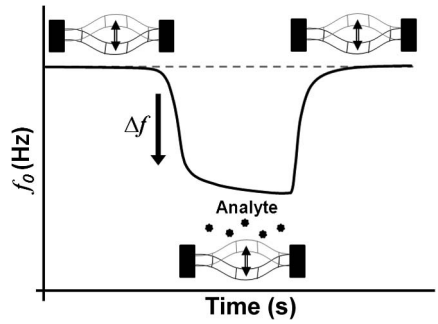

Fig. 1. Conceptual diagram of transient frequency shift of a resonant chemical sensor based on mass loading.

Among these resonant sensors, the CMUT sensor is a promising platform for practical and versatile applications because of its high mass sensitivity, its multiresonant array structure, and a high quality factor. Using the 50-MHz CMUT sensor with a mass sensitivity at the zeptogram range $(\sim 10^{-21})$, the state-of-the-art volume sensitivity and resolution to dimethyl methylphosphonate, a common simulant for sarin gas, have been demonstrated for homeland security applications [9], [12]. In addition, the versatility of the CMUT as a chemical sensor has been demonstrated through the detection of volatile organic compounds [13], detection of carbon dioxide (CO_2) and relative humidity for environmental monitoring applications [14], and detection of antibodies for biomedical applications [15].

A practical resonant sensor system requires not only a highly sensitive resonant device, such as the CMUT, but also an appropriate circuit to interface with the sensor. Sensor interface circuits dictate how the information is delivered to the end user and they often contribute to the system noise [16], [17], i.e., a low-noise oscillator circuit is key in achieving a high sensor resolution. Various oscillator topologies, such as single-stage tuned oscillators or amplifier-based series oscillators, have been used for resonant devices, such as Quartz, FBARs, and SAWs. However, these oscillator topologies are not suitable for the CMUT sensor because of three constraints: common ground between sensors, higher Q at parallel resonant frequency, and requirement for a high gain from the oscillator. Thus, a different oscillator topology must be explored for the CMUT sensors.

Manuscript received July 12, 2012; revised January 21, 2013 and May 21, 2013; accepted July 15, 2013. Date of publication January 14, 2014; date of current version May 2, 2014. This work was supported in part by Silicon Valley Laboratory, Texas Instruments, Santa Clara, CA 95051 USA; and in part by the Korea Institute of Science and Technology Institutional Program (2E23880), the Original Technology Research Program for Brain Science through the National Research Foundation of Korea funded by the Ministry of Education, Science, and Technology (2012M3C7A1055410).

H. J. Lee was with the Department of Electrical Engineering, Stanford University, Stanford, CA 94305 USA. She is now with the Korea Institute of Science and Technology, Seoul 136-791, Korea (e-mail: hyunjoo.lee@kist.re.kr).

K. K. Park is with the Department of Mechanical Engineering, Hanyang University, Seoul 133-791, Korea (e-mail: kwankyu@hanyang.ac.kr).

Ö. Oralkan is with the Department of Electrical and Computer Engineering, North Carolina State University, Raleigh, NC 27695 USA (e-mail: omer.oralkan@ncsu.edu).

M. Kupnik is with the Department of Electrical Engineering, Brandenburg University of Technology, 03046 Cottbus, Germany (e-mail: kupnik@tu-cottbus.de).

B. T. Khuri-Yakub is with the Department of Electrical Engineering, Stanford University, Stanford, CA 94305 USA (e-mail: khuri-yakub@stanford.edu).

Digital Object Identifier 10.1109/TIE.2014.2300031

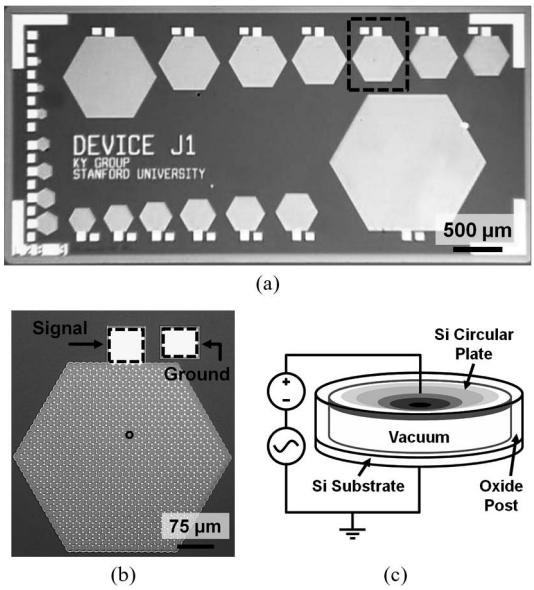

Fig. 2. Photographs of (a) a die of a CMUT array and (b) a CMUT resonant sensor with 817 circular cells. (c) Schematic diagram of bias scheme for a single circular CMUT resonator.

In addition, multichannel capability is beneficial to accommodate an array of resonant sensors. A resonant sensor based on the mass-loading mechanism not only detects the change in mass due to the analyte of interest but also responds to environmental changes, such as temperature and pressure fluctuations. One solution to address this issue is the use of an array of resonant sensors to perform pattern recognition [18], [19], which requires multichannel interface circuits. A multichannel implementation, however, requires more area and many electrical connections when implemented using discrete electronic components. Another challenge with the multichannel detection is the potential frequency locking (i.e., channels oscillating at the same frequency) between channels [13].

Thus, in this paper, we present a multichannel interface integrated circuit (IC), designed specifically for an array of 50-MHz CMUT sensors. Each channel contains a low-noise oscillator that tracks the resonant frequency of a single CMUT sensor in real time and an output buffer. The IC, which was implemented in a 0.18-μm CMOS technology, significantly improved our sensor system in terms of area and power consumption compared to the previous implementation using discrete electronic components [9]. In addition, the frequency-locking problem was solved by designing the gain of the amplifiers in the oscillator loop to be adjustable off-chip using an external voltage. The operation of the developed interface IC for CMUT resonant sensors was demonstrated through two-channel detection of relative humidity.

II. Sensor and Operational Principle

A. Structure of the CMUT Resonant Sensor

A 2.5-mm-by-5-mm die consists of 22 CMUT resonant sensors in an array structure to allow multichannel detection [Fig. 2(a)]. These sensors share a common ground through the conductive silicon substrate. A single CMUT resonant sensor is composed of hundreds to thousands of identical circular resonators, which are all electrically connected in parallel through the top electrode [Fig. 2(b)]. The number of resonators n in each device was varied in this design to experiment with different device input impedance values. When n resonators are connected in parallel, the motional impedance is reduced by a factor of n, and the thermal noise is hence reduced by a factor of $\sqrt{n}$ [20]. Thus, this multiresonator configuration is beneficial in achieving a low minimum level of detection (LOD), i.e., improving the resolution of the sensor system. The individual resonator in the multiresonator configuration is a parallel-plate capacitor with a circular single-crystal silicon plate [Fig. 2(c)]. The first flexural-mode resonant frequency of this circular plate is defined by [21]

$$f_0 = \frac{0.83}{a}\sqrt{\frac{Et^3}{m(1-v^2)}} \tag{1}$$

where a is the radius, E is Young's modulus (tensile modulus) of silicon, t is the thickness, v is the Poisson ratio, and m is the mass of the circular plate. A high mechanical resonant frequency of $\sim$50 MHz was achieved with a plate radius of 5.3 μm and a plate thickness of 500 nm. Details of the CMUT fabrication, structure, and various characterizations have been described previously [22].

The CMUT-based resonators offer two main advantages for the resonant sensor applications: high quality factor and compatibility for versatile chemical functionalization. The vacuum-sealed cavity eliminates the damping from the backside of the flexural-mode resonant plate. Thus, the quality factor (Q) of such a structure at the fundamental mode is higher than that of other flexural-mode resonators when the conditions such as materials, thickness, and detection area (i.e., $\sim 88\ \mu\text{m}^2$) are the same [23]–[26]. In addition, because the backside of the resonant plate is protected by the vacuum-sealed cavity, various methods of chemical functionalization such as spin coating and dip coating can be adopted. In comparison to chemical sensor systems based on other electromechanical devices, such as bulk acoustic wave, SAW, and micro-/nanocantilevers, the sensor system based on CMUTs has been demonstrated to offer the best sensitivity and LOD to formaldehyde and CO_2 [12].

B. Electrical Characterization of the CMUT Resonant Sensor

The resonant characteristics of CMUTs used in this study were measured by using an impedance analyzer (Agilent Technologies, Model 4294A, Palo Alto, CA, USA). The CMUTs were biased at different dc voltages, and the impedance analyzer provided a sinusoidal ac signal with an amplitude of 50 mV_{rms}. As the dc voltage increased, the resonant frequency decreased due to the spring softening effect [27], as shown in Fig. 3(a). In the resonant sensor application, the CMUT is biased at a fixed dc voltage that results in a high quality factor. For example, 44 V was chosen as the operating voltage because the CMUT sensor exhibited a high quality factor of $\sim$300 at the parallel resonant frequency of 44.83 MHz. Close examination of the input impedance shows that the quality factor at the parallel resonant frequency ($\sim$300) is higher than that at the

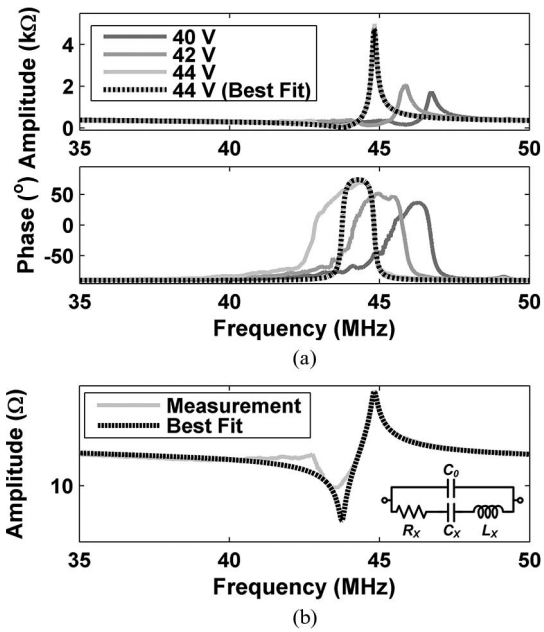

Fig. 3. (a) Measured input impedance of the CMUT (solid: measurement; dashed: best fit). (b) Zoom-in input impedance at a bias voltage of 44 V (inset: equivalent circuit model).

series resonant frequency (∼65) because the nonuniformity between resonators in the multiresonant structure of the CMUT is more visible at the series resonant frequency [Fig. 3(b)]. The conventional Butterworth van Dyke model [28] was used to fit the input impedance at a given dc bias voltage [Fig. 3(b) inset], which was used to design and simulate the free-running oscillator.

C. Operational Principle

Mass loading is the main operational principle of the CMUT chemical sensor. As estimated in (1), the resonant frequency of a circular plate decreases when the mass of the resonant structure increases. For chemical detection, the resonant structure is functionalized with a chemically sensitive layer to be sensitive to the analyte of interest. The analyte absorption results in an increase in the mass and thus a decrease in the frequency (Fig. 1).

The LOD of a resonant sensor (2) is estimated by differentiating (1), which indicates that the LOD is a function of both the mass sensitivity of the device and the frequency noise of the resonant sensor system (Δf), i.e.,

$$\Delta m = -2 \cdot \Delta f \cdot \frac{m}{f}. \tag{2}$$

As the 50-MHz CMUT offers an excellent mass sensitivity of 4.3 ag/Hz (or ~ 49 zg/Hz/μm^2), the sensor interface circuit must exhibit a good frequency noise performance.

III. Sensor Interface Circuitry

A four-channel oscillator circuit was designed and implemented in a 0.18-μm CMOS process to interface with the array of CMUT resonant sensors. The oscillator tracks the frequency shift due to mass loading in real time. The Allan deviation [29] was measured to estimate the noise floor and, thus, the resolution.

A. Oscillator Topology for CMUT Sensors

There are two characteristics of CMUTs that constrain the choice of the oscillator topology: First, the 22 CMUT sensors in a die share a common ground through the silicon substrate. Thus, for multichannel detection using CMUTs, topologies such as the Pierce oscillator [30] that require access to both electrodes of the individual resonator are not suitable. Second, the quality factor at the parallel resonance is often higher than that at the series resonance for the CMUTs because of the multiresonator configuration. Each resonator in the multiresonator configuration has a slightly different resonant frequency due to the errors incurred during the fabrication process. This resonator-to-resonator nonuniformity is more visible at the series resonance for CMUTs because the displacement is maximum at this frequency. Therefore, for such resonator arrays, we propose an oscillator topology that oscillates near the parallel resonance rather than at the series resonance, such as the Colpitts oscillator [30], to achieve a low-frequency noise.

There are two popular Colpitts oscillator topologies for MEMS resonators [31]: single-stage tuned and amplifier-based oscillators. The single-stage tuned oscillators offer the benefits of low power consumption and low noise but could suffer from an unreliable start-up behavior [31]. Oscillation will not start if the resonator is too lossy compared to the maximum negative resistance provided by a single-stage amplifier. In contrast, despite the potentially higher thermal noise and power consumption, the amplifier-based Colpitts oscillators are designed to guarantee a reliable start-up by providing enough gain (often higher than an open-loop gain of one) to satisfy the Barkhausen criteria at resonance. The CMUT, a flexural-mode resonator, is considered lossy as the topside of the resonant plate must be exposed to the medium for chemical detection and thus is subject to air damping. Therefore, we chose the amplifier-based Colpitts oscillator to ensure a reliable start-up behavior.

B. Design and Simulation of the Four-Channel Opamp-Based Oscillator

Our design approach for the amplifier-based Colpitts oscillator was to achieve an open-loop gain and phase shift near parallel resonance (∼50 MHz) to satisfy the Barkhausen criteria for oscillation: an open-loop gain of one and a phase shift of zero [Fig. 4(a)]. The open-loop characteristics were observed when the loop was opened at the X_A node. First, the CMUT is biased at a fixed dc voltage $(V_{\rm dc})$ through a bias network that is composed of R_B and C_B to prevent shortage and to decouple the dc voltage, respectively. The CMUT is then interfaced with the input of a gain stage through a capacitive divider. The value of the capacitor in the divider $(C_{\rm DIV,1})$ with respect to the device capacitance (C_0 or $C_{\rm DIV,2}$) is chosen to consider the tradeoff between gain and loading. For example, a large $C_{\rm DIV,1}$ will result in a large gain. However, the large $C_{\rm DIV,1}$ results in

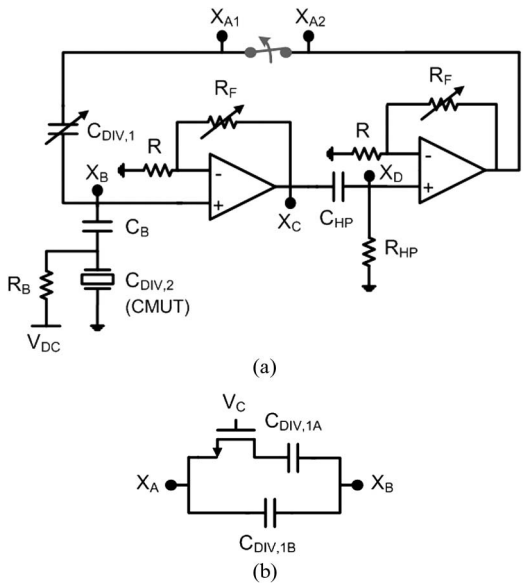

Fig. 4. (a) Block diagram of the opamp-based oscillator. (b) Schematic diagram of the variable capacitor.

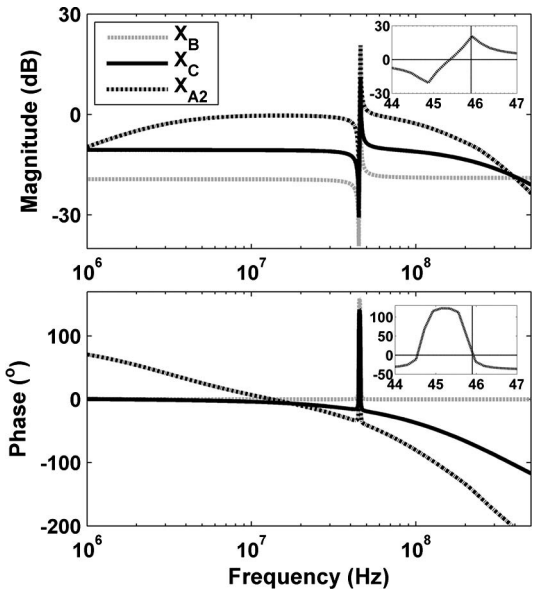

Fig. 5. Simulated open-loop ac magnitude and phase (inset: close-in plot where the frequencies are in megahertz).

a large loading across the CMUT, degrading the loaded quality factor. For this design, we added the flexibility to select between two $C_{\mathrm{DIV},1}$ values by adding a switch controlled by V_C at the secondary capacitor [Fig. 4(b)]. (An NMOS switch was chosen instead of a transmission gate mainly to save the die area as on-resistance value and charge injection are not critical in this design.) The main purpose of the added flexibility is to supply additional gain for a given CMUT.

In addition, the noise performance of the oscillator is important because the short-term frequency stability of the oscillator Δf determines the limit of detection Δm of a resonant sensor based on mass loading and, thus, the sensor resolution. When a resonant sensor is developed for an environment monitoring application to detect CO_2, a reasonable desired resolution is around 0.003%, an order of magnitude smaller than the CO_2 concentration in ambient. Based on the known volume sensitivities of CMUTs functionalized with chemically sensitive layers [14], the required frequency noise ranges from 18 to 40 Hz. Thus, the target specification for the frequency noise is set to 10 Hz. In effort to reduce the frequency noise and to meet this requirement, $C_{\mathrm{DIV},1}$ that minimizes the device loading (i.e., loaded Q) is chosen since the frequency noise is inversely proportional to Q.

The subsequent two stages were designed to provide sufficient gain, phase shift, and filtering for the loop condition to satisfy the Barkhausen criteria near the parallel resonance. The open-loop gain was designed to be larger than four near the parallel resonant frequency to achieve a reliable start-up [30]. In a self-sustaining oscillator with no input source, a thermal noise or a sudden voltage change in the resonator when powered is amplified through the loop by an excessive open-loop gain. The loop signal continues to increase until circuit nonlinearities such as amplifier saturation limit further amplification, and the effective loop gain reduces to one to achieve a stable oscillation. Thus, in our design, we aimed to achieve an excess loop gain larger than four.

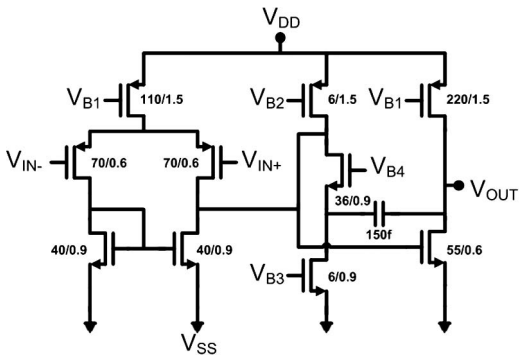

Fig. 6. Schematic diagram of two-stage OTA.

As the maximum closed-loop gain of our amplifier is approximately three when the 3-dB bandwidth is approximately 250 MHz, two amplifier stages are employed. The two noninverting gain stages serve as inherent low-pass filters due to the limited gain–bandwidth product of the amplifiers. The RC stage between these two stages serves as a high-pass filter. Overall, a broadband bandpass filter with a center frequency near the parallel resonance is achieved (Fig. 5). In addition, the gain of each stage was designed to be adjustable to allow oscillation for various 50-MHz CMUTs on the die with different quality factors and device capacitances (C_0). In the feedback loop, an NMOS resistor is used to achieve an adjustable feedback resistance. When the gate voltage of this NMOS resistor is increased from 2 to 2.5 V, the gain is adjusted from 3 to 1.8.

The basic block of the two gain stages and the buffer stage is a simple two-stage operational transconductance amplifier (OTA) optimized for low power consumption (Fig. 6). This OTA was designed to achieve a dc gain of 70 dB, a phase margin of 60°, and a 3-dB bandwidth of 800 MHz (Fig. 7). The bias for the current mirror is adopted from Steininger [32] with a start-up circuitry [33] (Fig. 8). For the output buffer stage, a source-follower stage is added to achieve low output impedance.

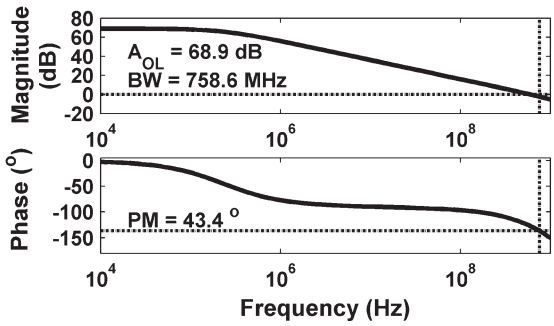

Fig. 7. Simulated ac open-loop characteristics of the OTA.

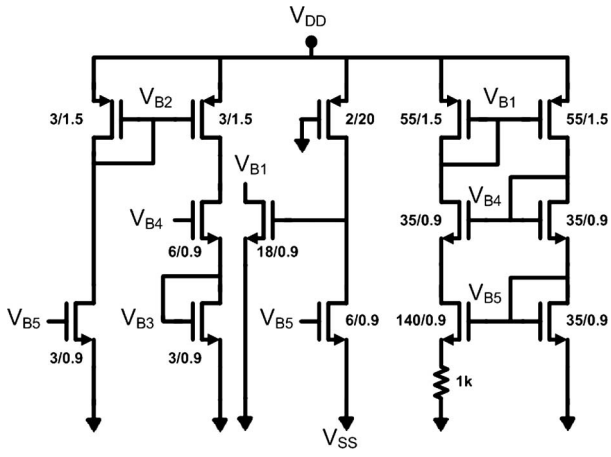

Fig. 8. Schematic diagram of current buffer with a start-up circuitry.

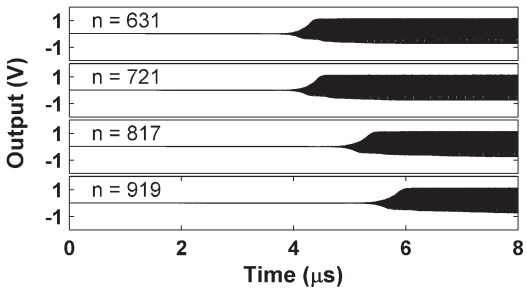

Fig. 9. Transient simulation.

The transient simulation was performed using Cadence Spectre. In the simulation, the oscillators were interfaced with equivalent circuit models of 50-MHz CMUTs biased at the same dc voltage of 50 V but with different sizes $(n = 631 \sim 919)$. A larger device (i.e., larger C_0) results in a smaller gain in the capacitor divider. Thus, for larger devices, the voltages across the NMOS resistors were decreased to increase the feedback resistances to compensate for the loss in the open-loop gain. When the gate voltage of the NMOS resistor is decreased from 2.5 to 2 V, the on-resistance was designed to increase from 0.9 to 1.5 kΩ (R in the feedback of each amplifier stage [Fig. 4(a)] is 500 Ω). All four oscillators successfully started up, demonstrating the functionality of the designed oscillator for various impedance sets of 50-MHz CMUTs (Fig. 9). The start-up time for the larger devices ($n = 817$, 919) is longer, however, because the open-loop gain cannot be increased indefinitely.

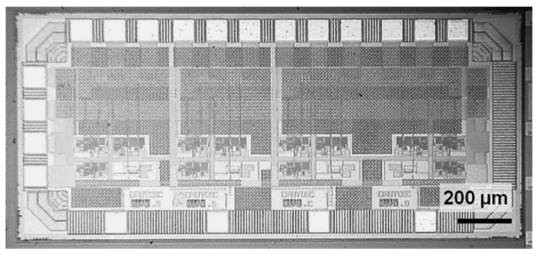

Fig. 10. Die photograph of the IC.

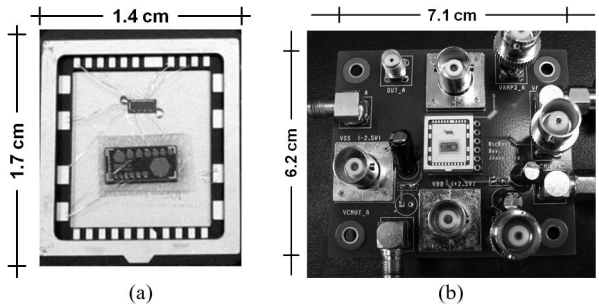

Fig. 11. Photographs of (a) chip carrier and (b) PCB.

Four identical amplifier-based Colpitts oscillators for ∼50-MHz CMUTs were designed and fabricated in the 0.18-μm CMOS technology with ±2.5-V supply voltage (Fig. 10). These oscillators share power, ground, and a voltage line to select the divider capacitor (C_{DIV}), while they have separate ports for CMUT inputs, oscillator outputs, and voltages to adjust the amplifier gains.

C. Characterization of the Four-Channel Oscillator Chip

The test setup for the fabricated chip consists of a ceramic chip carrier to interface with the external circuitry and a printed circuit board (PCB) to connect to power supplies and frequency counters. The implemented application-specified integrated circuit chip and the CMUT die were mounted on the same chip carrier (1.7 cm × 1.4 cm) and were connected to the pads through Al bond wires [Fig. 11(a)]. For the purpose of characterization, a CMUT sensor $(n = 721)$ without a functionalization layer was used. On power-up, the gate voltages of NMOS resistors in the feedback of two amplifiers were initially set at 2 V. The feedback resistance of one of the amplifiers was then reduced until an oscillation is observed.

The noise of the oscillator was estimated in the time domain using the Allan deviation [29]. We used a frequency counter (Stanford Research Systems, Model SR620, Sunnyvale, CA, USA) to compute the overlapped Allan deviation from the data collected at a sampling rate of 200 Hz. The Allan deviation at different averaging times shows the lowest Allan deviation of 9.72×10^{-8} at an averaging time of 2 s and a corresponding frequency noise of 4.34 Hz (1σ) (Fig. 12). (This frequency noise is ten times higher than that of a circuit implemented using discrete components [9] since this circuit consumes less power [29], [34] but is still low enough to achieve a high sensor resolution.)

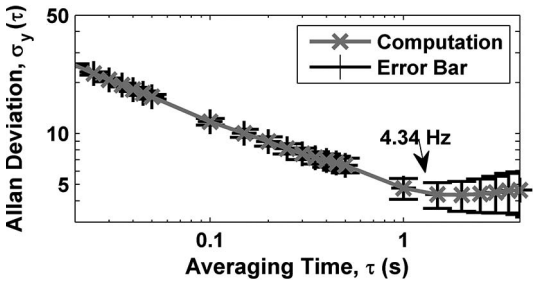

Fig. 12. Allan deviation.

TABLE I
IC OSCILLATOR PERFORMANCE SUMMARY

Technology	0.18 μm CMOS
Supply voltage	±2.5 V
Power dissipation	72.5 mW/channel
Output oscillation frequency	44.63 MHz (CMUT: 44 V)
Frequency noise	4.34 Hz (1σ)
Circuit area	1940 μm × 930 μm

The IC implementation of the oscillators offers three advantages compared to the previous implementation using discrete electronic components: smaller footprint ($\sim$1.8 mm^2), lower power consumption, and capability to control frequency locking (Table I). The IC footprint for a single channel including IC pads (i.e., 485 μm × 930 μm or 0.45 mm^2) is $\sim$1300 times smaller than the footprint of the single-channel oscillator implemented using discrete electronic components (excluding external connectors for both cases). The power consumption per channel (i.e., 72.5 mW) is reduced by approximately ten times, which, in particular, is beneficial for a multichannel implementation (Table I).

In such a multichannel implementation, the issue of frequency locking between channels needs to be addressed. The frequency locking due to electrical and/or mechanical cross-coupling between CMUT resonators in the array can be prevented both in the device implementation and in the circuit design. Adding wafer isolation trenches between the resonators in the array is one method to reduce mechanical cross-coupling between adjacent resonators [13].

The presented circuit has a knob to adjust the open-loop gain for each oscillator which can be used to unlock the frequency output of one channel from the other. The resonant frequency of the CMUT is a function of bias voltage [Fig. 3(a)], and thus, one way to unlock is to adjust the bias voltage of one of the locked CMUT sensors. However, because Q and C_0 of the CMUTs are also functions of bias voltage, the open-loop gain must be compensated accordingly to sustain the oscillation. Without the capability to adjust the open-loop gain, the range of bias voltages allowed for an oscillation is limited, and the unlocking of two channels might not be possible. When two CMUT devices from an array without the wafer isolation trenches [Fig. 2(a)] were interfaced with the presented circuit, the frequency outputs of two channels were easily locked [Fig. 13(a)]. By adjusting the value of the feedback resistance of the amplifier stage in the oscillator loop and the CMUT bias voltages, both frequencies were modified. Both frequency outputs were measured over 5 h to confirm that the two frequencies did not merge back to the same frequency [Fig. 13(b)].

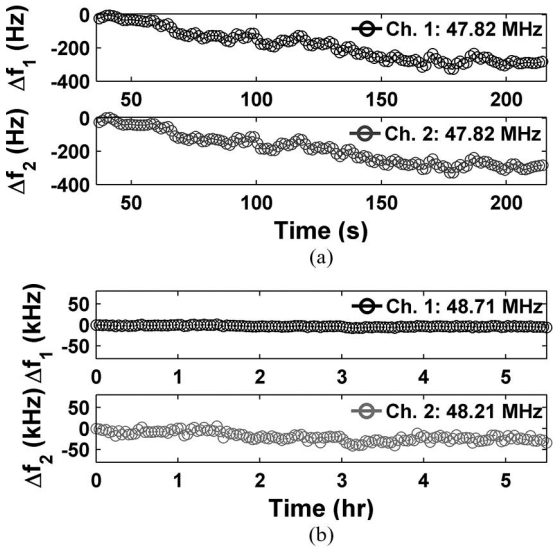

Fig. 13. Frequency outputs of two channels (a) locked and (b) unlocked.

IV. CHEMICAL RESULTS

A. Functionalization and Chemical Setup

The CMUT sensors were functionalized with an approximately 85-nm-thick mesoporous silica layer and an approximately 70-nm-thick guanidine polymer layer to enhance the sensitivity to water. Successful detections of CO_2 [14] and trinitrotoluene [35] were previously demonstrated using functionalized mesoporous silica as a chemically sensitive layer on resonant sensors. The mesoporous silica layer was self-assembled on top of the CMUT die using the evaporation-induced self-assembly method developed by Zhao *et al.* [14], [36]. The average measured frequency shift due to the addition of this functionalization layer was 1.3 MHz [14], which is within the reasonable range of estimated frequency shift of 1.16 MHz assuming 50% porosity. Guanidine polymer was prepared by mixing 20% aqueous polyhexamethylene biguanide (Arch Chemicals, Inc., Norwalk, CT, USA) in a solution that contains 50% isopropanol and 50% distilled water [37]. This mixture was applied on top of the CMUT using spin coating with a spin speed of 2000 r/min.

Different concentrations of water vapor were generated using the saturation bubbler method. A mass flow controller adjusts the flow rate of the carrier gas (dry N_2) that is injected into the bubbler. The saturated vapor generated from the bubbler is then merged back with the carrier gas. In this setup, we set the total flow rate of the final mixture to be constant. The final mixture is then delivered into a glass chamber (0.8 cm^3), which was custom designed to fit on top of the chip carrier to enclose the sensor.

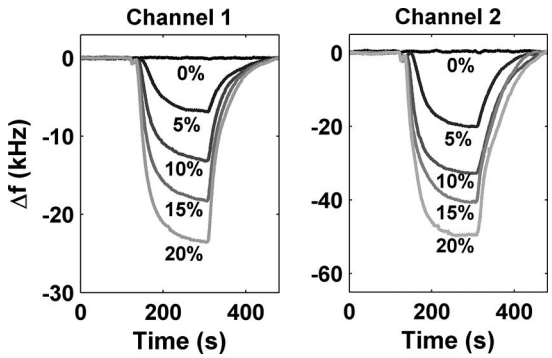

Fig. 14. Transient responses to relative humidity.

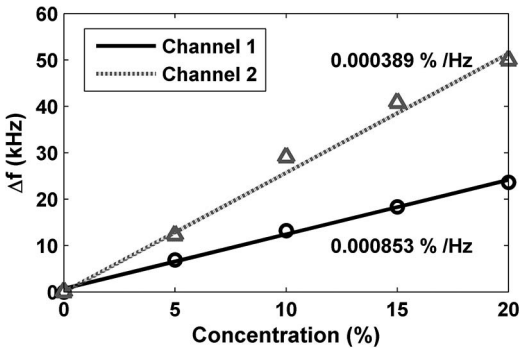

Fig. 15. Chemical sensitivity to relative humidity in N_2.

B. Results From Chemical Experiments

Transient responses of two functionalized sensors to various concentrations of water vapor from 0% to 20% were measured (Fig. 14). As predicted, the oscillation frequency began to decrease at 120 s when the relative humidity reacted with the chemically sensitive layer on top of the CMUT sensor. When the chamber was purged with the carrier gas at 300 s, the frequency recovered back to the baseline. The maximum frequency shifts at different concentrations are plotted, and the slope is estimated by using a best fit linear regression. The volume sensitivity is estimated by taking the inverse of this slope (Fig. 15).

The first sensor functionalized with mesoporous silica layer exhibited a volume sensitivity of $8.53 \times 10^{-4}\%/\text{Hz}$, while the second sensor functionalized with the guanidine polymer exhibited a volume sensitivity of $3.89 \times 10^{-4}\%/\text{Hz}$ ($\sim$2.2 times more sensitive). Although estimating the magnitudes of frequency shifts due to various relative humidity concentrations based on the chemical reaction is beyond the scope of this work, the measured volume sensitivities are found to be comparable to other resonant sensors, such as FBAR and SAW [14]. The volume resolutions derived using the Allan deviation (i.e., 3.7×10^{-3} and 1.7×10^{-3} Hz) are one of the lowest reported in the literature [14].

The different volume sensitivities demonstrate that the frequencies of two channels were not locked during the chemical experiment, and thus, the results can provide a useful set of information to a pattern recognition algorithm. In addition, the average fall and rise time constants to 90% of full responses for both channels were computed. The rise and fall time constants of channel 1 were 88 and 105 s, respectively, while that of channel 2 were 53 and 53 s, respectively. This information can be served as extra data for more accurate pattern recognition. The developed IC oscillators can thus be interfaced with an array of resonant sensors that are functionalized with different chemically sensitive layers. Demonstration of more chemical detections and pattern recognition using an array of sensors will be part of future work.

V. Discussion

In comparison to sensor systems based on other resonant structures, the CMUT-based chemical sensor system offers the advantages of high sensitivity, array structure for multichannel detection, and low thermal noise [9]. While the sensor systems based on SAW resonators are well established and offer the capability of dual channels, they suffer from the limitations of low sensitivity and relatively large size (approximately millimeters) [12]. FBARs operate at high resonant frequencies (approximately gigahertz), but the systems based on FBARs suffer from a high-frequency noise, resulting in low LOD (approximately ag/cm^2) [12]. Micro-/nanocantilevers are another promising sensor platforms which exhibit high sensitivity and are fabricated with a straightforward fabrication process. However, there are three distinctive disadvantages of cantilevers in comparison to CMUTs. First, to achieve a high mass sensitivity, the device dimension must be decreased further toward the nanometer regime [23], resulting in a small detection area. Second, both sides of the structure are exposed to air, and thus, consistent and uniform functionalization of such structure is challenging particularly in the nanometer regime. Finally, implementing an array of cantilevers for multichannel detection is challenging due to process variations.

Although the CMUT is a promising candidate for a portable chemical sensor system, there are still issues that need to be addressed and resolved in the future. For example, the presented sensor system does not address frequency drifts due to the changes in temperature and pressure in ambient. The measured temperature sensitivity of the 50-MHz CMUT was -1.59 kHz/°C(-32.6 ppm/°C), which is high enough to require for a temperature compensation scheme. One possible solution to compensate for the temperature and pressure fluctuations is to use a lookup table or a reference channel with a bare CMUT.

Another limitation of the presented system lies in further increasing the number of channels, which requires a large number of power supplies. The current system requires a power supply per CMUT sensor to provide the dc bias voltage and additional power supplies to adjust the open-loop gain. One potential method to minimize the power supply is to use a single power supply for all the CMUT devices by improving the open-loop gain adjustment scheme, which is part of future work. Implementing a scheme to adjust the open-loop gain, on-chip, not only would save the number of power supplies but also would be more practical. One potential solution is to implement an automatic gain control (AGC) circuit to restore the oscillation amplitude [38]. The AGC circuit not only compensates for the gain changes due to temperature drifts but also helps to reduce the distortion of the sinusoidal output.

VI. Conclusion

By developing four identical amplifier-based oscillators for ∼50-MHz CMUTs in a 0.18-μm CMOS technology, we have demonstrated ∼1300 and ∼10 times reductions in circuit footprint and power consumption per channel, respectively. Furthermore, we have addressed the potential-frequency-locking problem between channels by allowing the open-loop gain to be adjustable off-chip. We have demonstrated the feasibility of the developed oscillator for the chemical resonant applications for the CMUT sensors. Two channels that were operated simultaneously achieved excellent volume sensitivity and resolution to relative humidity. By resolving the concerns on the increase in the power consumption, the number of external electrical connections, and footprint area, the presented IC enabled the multichannel detection of a CMUT sensor array, a promising candidate for the future miniaturized chemical sensor system.

References

[1] F. J. Delgado, J. M. Quero, J. Garcia, C. L. Tarrida, P. R. Ortega, and S. Bermejo, "Accurate and wide-field-of-view MEMS-based sun sensor for industrial applications," *IEEE Trans. Ind. Electron.*, vol. 59, no. 12, pp. 4871–4880, Dec. 2012.

[2] N. Abbate, A. Basile, A. C. Faulisi, S. Sessa, and C. M. N. Brigante, "Towards miniaturization of a MEMS-based wearable motion capture system," *IEEE Trans. Ind. Electron.*, vol. 58, no. 8, pp. 3234–3241, Aug. 2011.

[3] R. N. Dean, A. Anderson, S. J. Reeves, G. T. Flowers, and A. S. Hodel, "Electrical noise in MEMS capacitive elements resulting from environmental mechanical vibrations in harsh environments," *IEEE Trans. Ind. Electron.*, vol. 58, no. 7, pp. 2697–2705, Jul. 2011.

[4] L. Lijie and D. Uttamchandani, "Flip-chip distributed MEMS transmission lines (DMTLs) for biosensing applications," *IEEE Trans. Ind. Electron.*, vol. 56, no. 4, pp. 986–990, Apr. 2009.

[5] R. Smith, D. R. Sparks, D. Riley, and N. Najafi, "A MEMS-based Coriolis mass flow sensor for industrial applications," *IEEE Trans. Ind. Electron.*, vol. 56, no. 4, pp. 1066–1071, Apr. 2009.

[6] N. V. Kirianaki, S. Y. Yurish, N. O. Shpak, and V. P. Deynega, "Smart sensors for electrical and non-electrical, physical and chemical variables: Tendencies and perspectives," in *Data Acquisition and Signal Processing for Smart Sensors*, 1st ed. Hoboken, NJ, USA: Wiley, 2002, pp. 3–5.

[7] R. Gabl, E. Green, M. Schreiter, H. D. Feucht, H. Zeininger, R. Primig, and D. Pitzer, "Novel integrated FBAR sensors: A universal platform for bio- and gas detection," in *Proc. IEEE Sensors*, 2003, vol. 2, pp. 1184–1188.

[8] A. E. Hoyt, A. J. Ricco, J. W. Bartholomew, and G. C. Osbourn, "SAW sensors for the room-temperature measurement of CO_2 and relative humidity," *Anal. Chem.*, vol. 70, no. 7, pp. 2137–2145, 1998.

[9] H. J. Lee, K. K. Park, M. Kupnik, Ö. Oralkan, and B. T. Khuri-Yakub, "Chemical vapor detection using a capacitive micromachined ultrasonic transducer," *Anal. Chem.*, vol. 83, no. 24, pp. 9314–9320, 2011.

[10] H. Yu, P. Xu, X. Xia, D.-W. Lee, and X. Li, "Micro-/nanocombined gas sensors with functionalized mesoporous thin film self-assembled in batches onto resonant cantilevers," *IEEE Trans. Ind. Electron.*, vol. 59, no. 12, pp. 4881–4887, Dec. 2012.

[11] M. Li, E. B. Myrs, H. X. Tang, S. J. Aldridge, H. C. McCaig, J. H. Whiting, R. J. Simonson, N. S. Lewis, and M. L. Roukes, "Nanoelectromechanical resonator arrays for ultrafast, gas-phase chromatographic chemical analysis," *Nano Lett.*, vol. 10, no. 10, pp. 3899–3903, 2010.

[12] S. Fanget, S. Hentz, P. Puget, J. Arcamone, M. Martheron, E. Colinet, P. Andreucci, L. Duraffourg, E. Myers, and M. L. Roukes, "Gas sensors based on gravimetric detection—A review," *Sens. Actuators B, Chem.*, vol. 160, no. 1, pp. 804–821, Dec. 2011.

[13] K. K. Park, H. J. Lee, G. G. Yaralioglu, Ö. Oralkan, M. Kupnik, C. F. Quate, B. T. Khuri-Yakub, T. Braun, H. P. Lang, M. Hegner, C. Gerber, and J. Gimzewski, "Capacitive micromachined ultrasonic transducers for chemical detection in nitrogen," *Appl. Phys. Lett.*, vol. 91, no. 9, pp. 094102-1–094102-3, Aug. 2007.

[14] H. J. Lee, K. K. Park, M. Kupnik, N. A. Melosh, and B. T. Khuri-Yakub, "Mesoporous thin-film on highly-sensitive resonant chemical sensor for relative humidity and CO_2 detection," *Anal. Chem.*, vol. 84, no. 7, pp. 3063–3066, 2012.

[15] A. Ramanaviciene, D. Virzonis, G. Vanagas, and A. Ramanavicius, "Capacitive micromachined ultrasound transducer (cMUT) for immunosensor design," *Analyst*, vol. 135, pp. 1531–1534, 2010.

[16] M. R. Nabavi and S. Nihtianov, "Eddy-current sensor interface for advanced industrial applications," *IEEE Trans. Ind. Electron.*, vol. 58, no. 9, pp. 4414–4423, Sep. 2011.

[17] S.-C. Jung, M.-S. Kim, and Y. Yang, "Baseband noise reduction method using captured TX signal for UHF RFID reader applications," *IEEE Trans. Ind. Electron.*, vol. 59, no. 1, pp. 592–598, Jan. 2012.

[18] H. K. Chan, "A low-cost integrated approach for balancing an array of piezoresistive sensors for mass production applications," *IEEE Trans. Ind. Electron.*, vol. 55, no. 2, pp. 937–940, Feb. 2008.

[19] A. V. Fernandes, V. F. Cardoso, J. G. Rocha, J. Cabral, and G. Minas, "Smart-optical detector CMOS array for biochemical parameters analysis in physiological fluids," *IEEE Trans. Ind. Electron.*, vol. 55, no. 9, pp. 3192–3200, Sep. 2008.

[20] J. R. Vig and Y. Kim, "Noise in microelectromechanical system resonators," *IEEE Trans. Ultrason., Ferroelectr., Freq. Control*, vol. 46, no. 6, pp. 1558–1565, Nov. 1999.

[21] L. Meirovitch, *Analytical Methods in Vibrations,* 1st ed. New York, NY, USA: Macmillan, 1967.

[22] K. K. Park, H. J. Lee, M. Kupnik, and B. T. Khuri-Yakub, "Fabrication of capacitive micromachined ultrasonic transducers via local oxidation and direct wafer bonding," *J. Microelectromech. Syst.*, vol. 20, no. 1, pp. 95–103, Feb. 2011.

[23] M. Li, H. X. Tang, and M. L. Roukes, "Ultra-sensitive NEMS-based cantilevers for sensing, scanned probe and very high-frequency applications," *Nat. Nanotechnol.*, vol. 2, pp. 114–120, 2007.

[24] K. Naeli and O. Brand, "Dimensional considerations in achieving large quality factors for resonant silicon cantilevers in air," *J. App. Phys.*, vol. 105, no. 1, pp. 014908-1–014908-10, Jan. 2009.

[25] F. R. Blom, S. Bouwstra, M. Elwenspoek, and J. H. J. Fluitman, "Dependence of the quality factor of micromachined silicon beam resonators on pressure and geometry," *J. Vac. Sci. Technol. B, Microelectron.*, vol. 10, no. 1, pp. 19–26, 1992.

[26] K. K. Park, H. J. Lee, P. Cristman, M. Kupnik, Ö. Oralkan, and B. T. Khuri-Yakub, "Optimum design of circular CMUT membranes for high quality factor in air," in *Proc. IEEE Ultrason. Symp.*, Beijing, China, 2008, pp. 504–507.

[27] W. P. Mason, *Electromechonical Transducers and VME Filters,* 1st ed. Princeton, NJ, USA: D. Van Nostrand Company Inc., 1948.

[28] S. Sherrit, H. D. Wiederick, and B. K. Mukherjee, "Accurate equivalent circuits for unloaded piezoelectric resonators," in *Proc. IEEE Ultrason. Symp.*, 1997, pp. 931–935.

[29] D. W. Allan, "Time and frequency (time-domain) characterization, estimation, prediction of precision clocks and oscillators," *IEEE Trans. Ultrason., Ferroelectr., Freq. Control*, vol. 34, no. 6, pp. 647–654, Nov. 1987.

[30] B. Razavi, *Design of Analog CMOS Integrated Circuits,* 1st ed. New York, NY, USA: McGraw-Hill, 2000.

[31] T. S. A. Wong and M. Palaniapan, "Micromechanical oscillator circuits: Theory and analysis," *Analog Integr. Circuits Signal Process.*, vol. 59, no. 1, pp. 21–30, Apr. 2009.

[32] J. M. Steininger, "Understanding wide-band MOS transistors," *IEEE Circuits Devices*, vol. 6, no. 3, pp. 26–31, May 1990.

[33] D. A. Johns and K. Martin, "Advanced current mirrors and opamps," in *Analog Integrated Circuit Design*, 1st ed. Hoboken, NJ, USA: Wiley, 1996, pp. 259–261.

[34] T. H. Lee and A. Hajimiri, "Oscillator phase noise: A tutorial," *IEEE J. Solid-State Circuits*, vol. 35, no. 3, pp. 326–336, Mar. 2000.

[35] P. Xu, H. Yu, and X. Li, "Functionalized mesoporous silica for microgravimetric sensing of trace chemical vapors," *Anal. Chem.*, vol. 83, no. 9, pp. 3448–3454, 2011.

[36] D. Zhao, P. Yang, N. Melosh, J. Feng, B. F. Chmelka, and G. D. Stucky, "Continuous mesoporous silica films with highly ordered large pore structures," *Adv. Mater.*, vol. 10, no. 16, pp. 1380–1385, Nov. 1998.

[37] H. J. Lee, K. K. Park, M. Kupnik, and B. T. Khuri-Yakub, "Functionalization layers for CO_2 sensing using capacitive micromachined ultrasonic transducers," *Sens. Actuators B, Chem.*, vol. 174, pp. 87–93, Nov. 2012.

[38] A. Zanchi, C. Samori, A. L. Lacaita, and S. Levantino, "Impact of AAC design on phase noise performance of VCOs," *IEEE T Circuits-II*, vol. 48, no. 6, pp. 537–547, Jun. 2001.

Hyunjoo Jenny Lee (S'04–M'13) received the B.S. degree in electrical engineering and computer science, and the M.Eng. degree in electrical engineering from the Massachusetts Institute of Technology (MIT), Cambridge, MA, USA, in 2004 and 2005, respectively, and the Ph.D. degree in electrical engineering from Stanford University, Stanford, CA, USA, in 2012.

From 2004 to 2005, she was an MIT VI-A Fellow with Analog Devices, Inc., Wilmington, MA, USA, where she studied continuous-time signal-delta analog-to-digital converters. From 2008 to 2011, she was an Engineering Intern at National Semiconductor, Santa Clara, CA, USA (now, TI Silicon Valley Laboratories, Texas Instruments). Since 2013, she has been a Research Scientist with the Brain Science Institute, Korea Institute of Science and Technology, Seoul, Korea. Her current research focuses on bio-/neuromicroelectromechanical systems, particularly on biosensing/chemical sensing, sensor interface circuit design, multifunctional neural probe, and neuromodulation.

Dr. Lee is also a member of the Eta Kappa Nu and Tau Beta Pi honor societies.

Kwan Kyu Park (S'10–M'12) received the B.S. degree in mechanical and aerospace engineering from Seoul National University, Seoul, Korea, in 2001, and the M.S. and Ph.D. degrees in mechanical engineering from Stanford University, Stanford, CA, USA, in 2007 and 2011, respectively.

From 2011 to 2013, he was a Research Associate with the Edward L. Ginzton Laboratory, Stanford University. He is currently an Assistant Professor with the Department of Mechanical Engineering, Hanyang University, Seoul, Korea. His research interests include chemical sensors/biosensors based on micromechanical resonators, multiresonator systems, charging of microelectromechanical systems (MEMS) devices, ultrasonic transducers, and RF MEMS.

Ömer Oralkan (S'93–M'05–SM'10) received the B.S. degree in electrical engineering from Bilkent University, Ankara, Turkey, in 1995; the M.S. degree in electrical engineering from Clemson University, Clemson, SC, USA, in 1997; and the Ph.D. degree in electrical engineering from Stanford University, Stanford, CA, USA, in 2004.

He was a Research Associate (2004–2007) and then a Senior Research Associate (2007–2011) with the E. L. Ginzton Laboratory, Stanford University, and an Adjunct Lecturer (2009–2011) with the Department of Electrical Engineering, Santa Clara University, Santa Clara, CA, USA. Since 2012, he has been an Associate Professor with the Department of Electrical and Computer Engineering, North Carolina State University, Raleigh, NC, USA. He has authored more than 130 scientific publications. His current research focuses on developing devices and systems for ultrasound imaging, photoacoustic imaging, image-guided therapy, biological and chemical sensing, and ultrasound neural stimulation.

Dr. Oralkan is an Associate Editor for the IEEE TRANSACTIONS ON ULTRASONICS, FERROELECTRICS, AND FREQUENCY CONTROL, and serves on the Technical Program Committee of the IEEE Ultrasonics Symposium. He was the recipient of the 2013 Defense Advanced Research Projects Agency Young Faculty Award and the 2002 Outstanding Paper Award of the IEEE Ultrasonics, Ferroelectrics, and Frequency Control Society.

Mario Kupnik (SM'09) received the Diplom Ingenieur degree in electrical engineering from the Graz University of Technology, Graz, Austria, in 2000, and the Ph.D. degree in electrical engineering from the University of Leoben, Leoben, Austria, in 2004.

Before his Ph.D. studies (2000–2004), he was with Infineon Technologies AG, Graz, where he worked as an Analog Design Engineer in the field of ferroelectric memories and contactless smart card systems. From 2005 to 2011, he was a Postdoctoral Researcher, a Research Associate, and a Senior Research Scientist with the Edward L. Ginzton Laboratory, Stanford University, Stanford, CA, USA. Since March 2011, he has been a chaired Professor of Electrical Engineering with Brandenburg University of Technology, Cottbus, Germany.

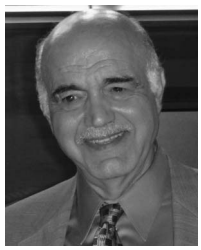

Butrus (Pierre) T. Khuri-Yakub (S'70–M'76–SM'87–F'95) received the B.S. degree in electrical engineering from the American University of Beirut, Beirut, Lebanon, in 1970; the M.S. degree in electrical engineering from Dartmouth College, Hanover, NH, USA, in 1972; and the Ph.D. degree in electrical engineering from Stanford University, Stanford, CA, USA.

He is currently a Professor of Electrical Engineering with Stanford University. He has authored over 550 publications and has been a principal inventor or coinventor of 92 US and international issued patents. His current research interests include medical ultrasound imaging and therapy, ultrasound neurostimulation, chemical/biological sensors, gas flow and energy flow sensing, micromachined ultrasonic transducers, and ultrasonic fluid ejectors.

Dr. Khuri-Yakub was the recipient of the Medal of the City of Bordeaux in 1983 for his contributions to nondestructive evaluation; the Distinguished Advisor Award from the School of Engineering, Stanford University, in 1987; the Distinguished Lecturer Award from the IEEE Ultrasonics, Ferroelectrics, and Frequency Control Society in 1999; a Stanford University Outstanding Inventor Award in 2004; a Distinguished Alumnus Award from the School of Engineering, American University of Beirut, in 2005; a Stanford Biodesign Certificate of Appreciation for Commitment to Educate, Mentor, and Inspire Biodesign Fellows in 2011; and the 2011 IEEE Rayleigh Award.